Penerbit Akademia Baru

Journal of Advanced Research in Fluid Mechanics and Thermal Sciences

Journal homepage: www.akademiabaru.com/arfmts.html
ISSN: 2289-7879

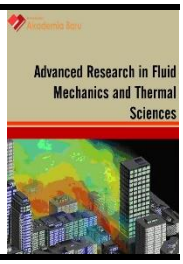

Numerical Investigation of Semi-Empirical Relation Representing Standard Deviation in Nusselt Profile Due to Water Jet Impingement

Open Access

Umair Siddique[1,*], Emaad Ansari[2], Sher Afghan Khan[3], Rajesh Patil[4]

[1] Department of Mechanical Engineering, Mukesh Patel School of Technology and Management, NMIMS University, Mumbai, India
[2] Department of Mechanical Engineering, MHSSCOE, Mumbai University, Mumbai, India
[3] Department of Mechanical Engineering, IIUM, Kuala Lumpur, Malaysia
[4] Department of Mechanical Engineering, Mukesh Patel School of Technology and Management, NMIMS University, Mumbai, India

ARTICLE INFO

Article history:
Received 6 August 2019
Received in revised form 18 October 2019
Accepted 29 October 2019
Available online 26 January 2020

Keywords:
Nusselt number; Reynolds number; nozzle-target spacing; standard deviation

ABSTRACT

Use of water jets in material processing industries is finding pace. Water jets are used for cooling of materials due to its high convective heat transfer coefficient. Nusselt number is the parameter used for studying the heat transfer rate through water jet impingement. Simulations are performed and Nusselt magnitudes are plotted for Reynolds number 2000, 2200, 2400, 2600, 2800, 3000, 3200 and 3400 at constant non-dimensional nozzle target spacing (z/d) 4. Also, Nusselt distribution is obtained at z/d = 1, 2, 3, 4, 5, 6, 7 and 8 at constant Reynolds value of 750. The standard deviation (STDEV) of Nusselt magnitude is arranged according to constant C (C = Re/ (z/d)) for regression analysis. The semi-empirical relation representing standard deviation (STDEV) in terms of C is found out to be $STDEV = 14.751 \times (C)^{0.917}$. Also, SST + Gamma-Theta turbulence model is found to predict accurate results.

1. Introduction

Cooling of hot surfaces using water jet impingement came into practice as the heat transfer rate due to air in some applications proved out to be insufficient. This is due to the fact that the heat transfer coefficient due of air is much smaller as compared to heat transfer coefficient of water. The local Nusselt magnitude which is a function of heat transfer coefficient is determined using the temperatures along the radial distance of the plate. The convective heat transfer which forms the major heat exchanging process in this phenomenon is widely dependent on Nusselt magnitude. Therefore, Nusselt profile is studied in this study and the standard deviation of local Nusselt magnitudes is evaluated at different parameters such as varying Reynolds number (Re) and varying non-dimensional nozzle target spacing (z/d). The magnitude of standard deviation (STDEV) is plotted against constant (C) which is a ratio of Re to z/d. Using the distribution of STDEV v/s C, semi-empirical

* *Corresponding author.*
E-mail address: umair.siddique@nmims.edu (Umair Siddique)

relations representing STDEV is proposed which is a function of C. Validation of the correlation is also conducted with the results of previous studies.

Umair and Gulhane [1] conducted experiments along with simulations to evaluate the constant representing the secondary peaks in the Nusselt profile due to air jet impingement. The constant was defined as ratio of Reynolds number of air to nozzle-target spacing and its value was found out to be 6000. Umair and Gulhane [2] carried out augmented study of heat transfer due to steady lateral air jet impinging on pin fin heat sink. The effect of various parameters on heat transfer rate was studied as well as best grid size and turbulence model was proposed. Umair and Gulhane [3] researched on the effect of different materials target surface on heat transfer due to air jet impingement. It was concluded that non-uniformity exists up to thermal diffusivity of 66.76 mm^2/s.

The effect of geometric thickness (t/d) of flat plate on cooling rate through plate was studied by Umair *et al.,* [4]. The non-uniformity in the Nusselt distribution profile was found to be below critical geometric thickness of 0.05. Umair *et al.,* [5] also evaluated the Nusselt magnitude at varying Reynolds number and z/d ratio and proposed correlations of Nusselt magnitude. Semi-empirical relations were proposed for r/d = 0, 0 < r/d < 1, 1 < r/d < 2.5 and r/d > 2.5. The correlations eliminate performing experiments and simulations to calculate the local Nusselt magnitude. Also, the critical range in the Nusselt distribution which is a product of Re and z/d within which secondary peaks rise were evaluated by Umair *et al.,* [6]. The range was found to be between 2205 and 2646000.

Similar to correlations for flat plate [5], semi-empirical relations representing local Nusselt value for pin fin heat sink was proposed by Umair *et al.,* [7]. The correlations were obtained by varying Reynolds number (Re), nozzle-target spacing (z/d), spacing of fin (S/d_p) and height of fin (H/d_p). Umair *et al.,* [8] also studied the heat transfer at lower nozzle spacing's. Power laws were proposed for the Nusselt distribution at lower z/d ratio. Augmented study of heat transfer due to pulse jet impinging on flat surface was also conducted by Umair *et al.,* [9]. G. no was proposed as a dimensionless number which governs the heat transfer due to pulse jet. Mark [10] studied heat transfer distribution due to steady air jet impinging on flat surfaces having different pattern. He observed the cooling characteristics under different parameters such as Reynolds number, nozzle-target spacing (z/d) and pattern of surfaces.

Khan *et al.,* [11] analysed threaded spikes numerically and found that it has no side effects on flow field and is efficient in base pressure control of bodies. Khan *et al.,* [12] created a semi-circular grooved cavity and concluded that it is a very effective passive control mechanism for base pressure regulations. Pathan *et al.,* [13] studied the effect of variations in base pressure on internal and external suddenly expanded flows and found that similar flow field is formed in internal and external expansion. Pathan *et al.,* [14] researched on the effectiveness of nozzle pressure ratio (NPR) and evaluated that with better NPR, base pressure gets reduced. Muhammed *et al.,* [15] focussed on the flow field around a non-circular cylinder and conclude that the pressure drag coefficient are in the range of 1 to 1.42. Convergent-divergent nozzle were studied for different area ratios by Khan *et al.,* [16]. It was found that area ratio plays an important role in base pressure distribution.

Webb and Ma [17] analysed heat transfer due to liquid jets of single phase. Water jets were also investigated by Webb and Ma [17] and the correlations representing Nusselt magnitude as a function of impinging parameters was reported. Wang *et al.,* [18] specifically used water jets of different flow rate to analyse the characteristics of heat transfer through hot plate.

The present study focusses on evaluating the semi-empirical relation representing the standard deviation (STDEV) in Nusselt magnitude due to water jet impinging on hot target surface which fills the gap between the literature studies and current work. A computational model is developed in ANSYS CFX solver over which grid independence test and turbulence modelling test is carried out. On achieving the best turbulence model a grid size at which results are independent, Nusselt variations

are plotted against r/d ratio by varying Reynolds number at constant r/d first and the by varying z/d at constant Reynolds number. The local Nusselt values obtained are then accumulated for different constant values (C = Re/ (z/d)). Regression analysis is carried out and a correlation is proposed for STDEV in terms of C.

2. Numerical Methodology

Figure 1 shows the computational model designed in ANSYS CFX solver that is used in simulation of the present study. An axis-symmetrical 2-D model was designed which consist of two domains namely solid domain and water domain. Water coming from nozzle impinges on hot target surface kept at constant heat flux of 1500 W/m^2. Temperature of water was set at 30℃. The water from nozzle travels through distance 'z' before impinging on surface and it radially flows outwards. The target surface length (L2) is 50mm. Four monitor points are set along radial distance 'r'. The local Nusselt magnitude is evaluated using Eq. (1) and Eq. (2).

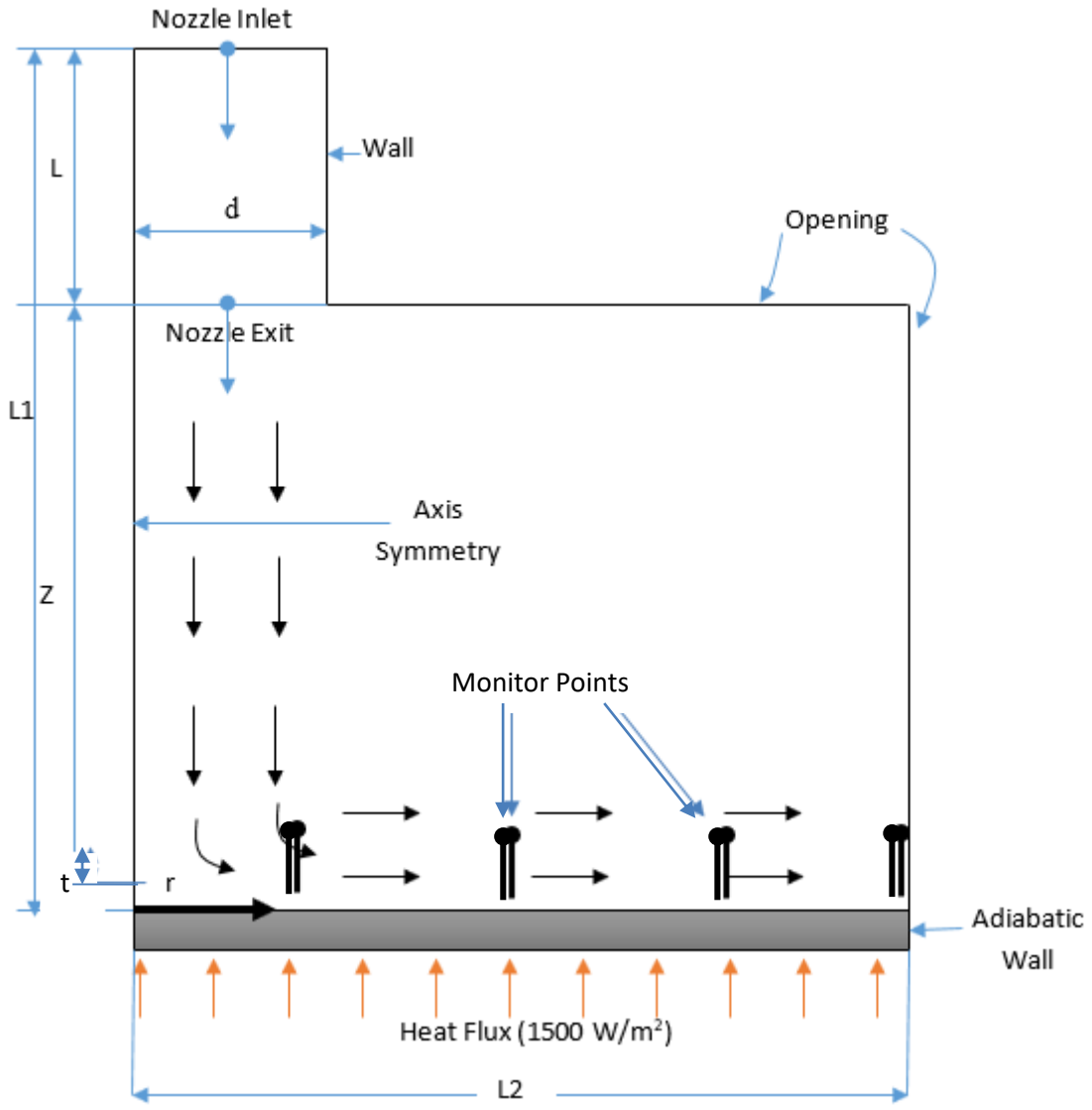

Fig. 1. Computational model

$$h = \frac{Q}{A \times (T_b - T_w)} \quad (1)$$

where,
h: Convective heat transfer coefficient
Q/A: Constant heat flux
T_b: Temperature of base plate
T_w: Temperature of water

$$Nu = h \times \frac{d}{K_w} \quad (2)$$

where,
Nu: Nusselt number
d: Diameter of nozzle
K_w: Thermal conductivity of water

2.1 Grid Independence Study

Grid independence test is carried out to obtain a computational grid that provides result independent of its size. The number of element used is 1000000, while the growth rate of L1 and L2 are varied for obtaining various grids. Images of growth rate 1.025, 1.05, 1.1, 1.125 and 1.2 are shown in Figure 2.

Figure 3 shows the Nusselt distribution at various growth rate. Growth rate sizes of 1.2, 1.175, 1.15, 1.125, 1.1, 1.075, 1.05 and 1.025 were used in the present study. The local Nusselt magnitude distribution at growth rate 1.05 and 1.025 has very small deviation. Thus, the computational model becomes independent of grid size at growth rate of 1.05. Hence, further simulations are carried out at growth rate of 1.05.

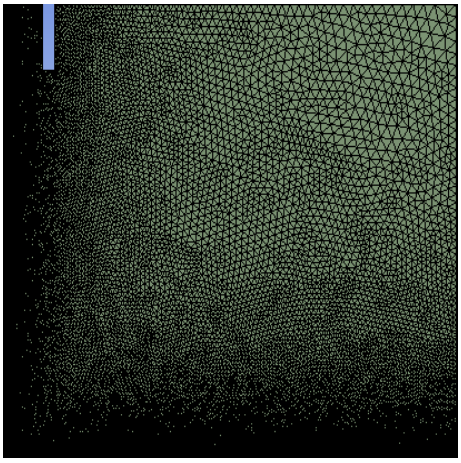

(a) Growth rate = 1.025

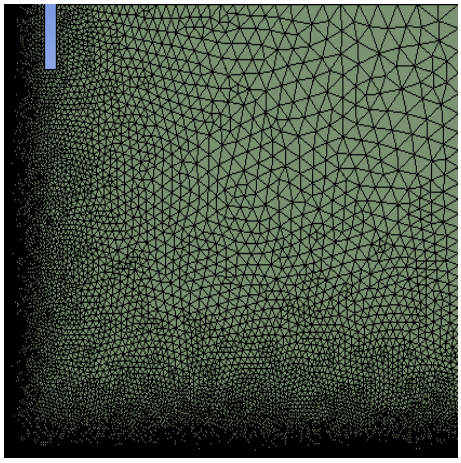

(b) Growth rate = 1.05

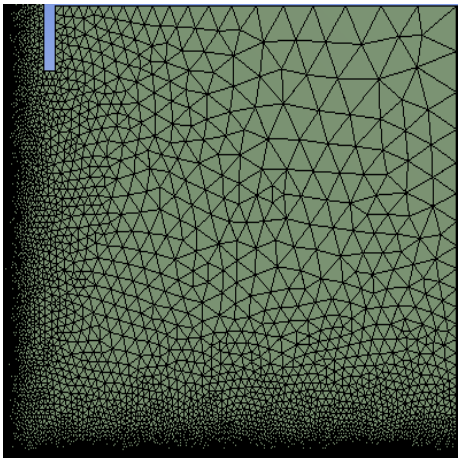

(c) Growth rate = 1.1

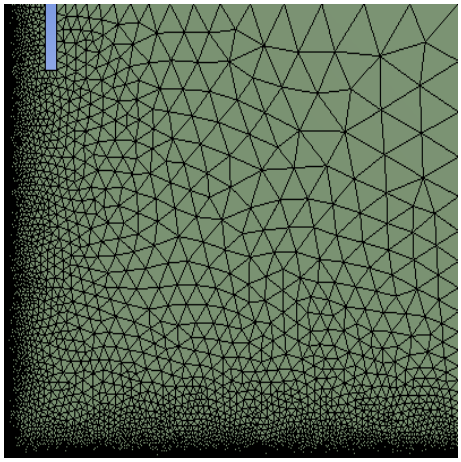

(d) Growth rate = 1.125

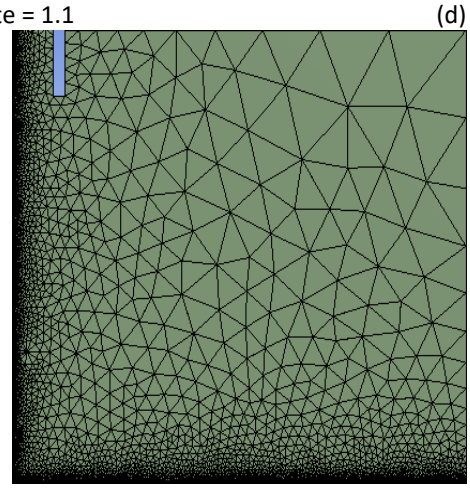

(e) Growth rate = 1.2

Fig. 2. Grid images at Growth rate 1.025, 1.05, 1.1, 1.125 and 1.2

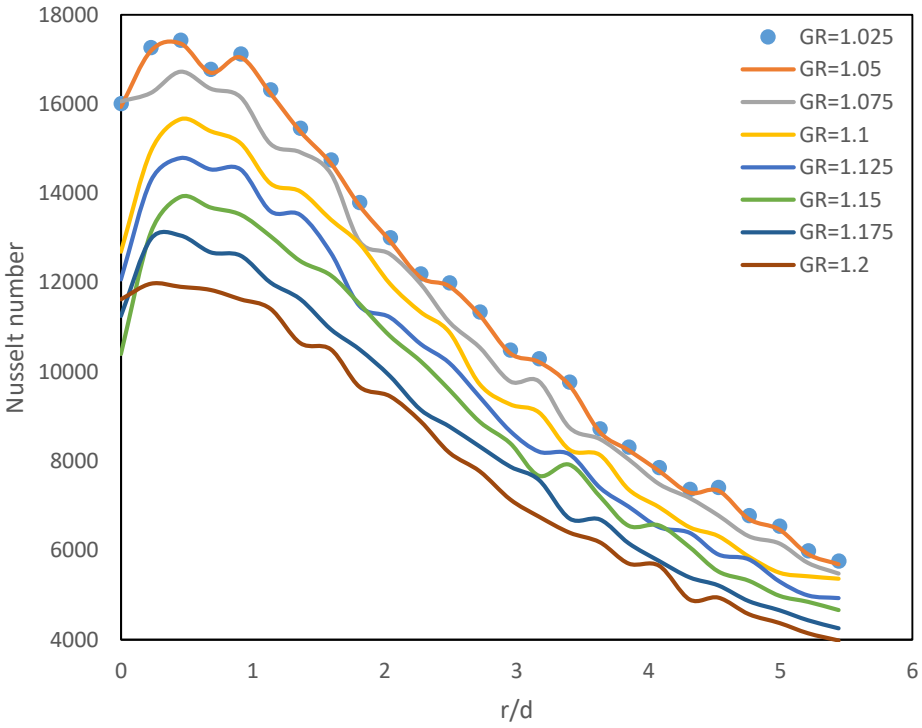

Fig. 3. Nusselt distribution at different Growth rate (1.025, 1.05, 1.075, 1.1, 1.125, 1.15, 1.175 and 1.2)

2.2 Turbulence Modelling

Computations are carried out at different turbulence models in the ANSYS CFX solver (Figure 4). Use of k-Epsilon model fetches better results in near jet (0 < r/d < 1) and far jet region (r/d > 1) while k-Omega provides better results of stagnation region. SST incorporates the use of both k-Epsilon and k-omega models but fails to capture the effects of intermediacy and onset transition. Hence, SST model is simultaneously used with Gamma-Theta model combination to provide accurate results. Thus, SST + Gamma – Theta turbulence model is used for simulations as it provides accurate results for near jet and far jet region along with incorporating the effect of intermediacy and onset transition.

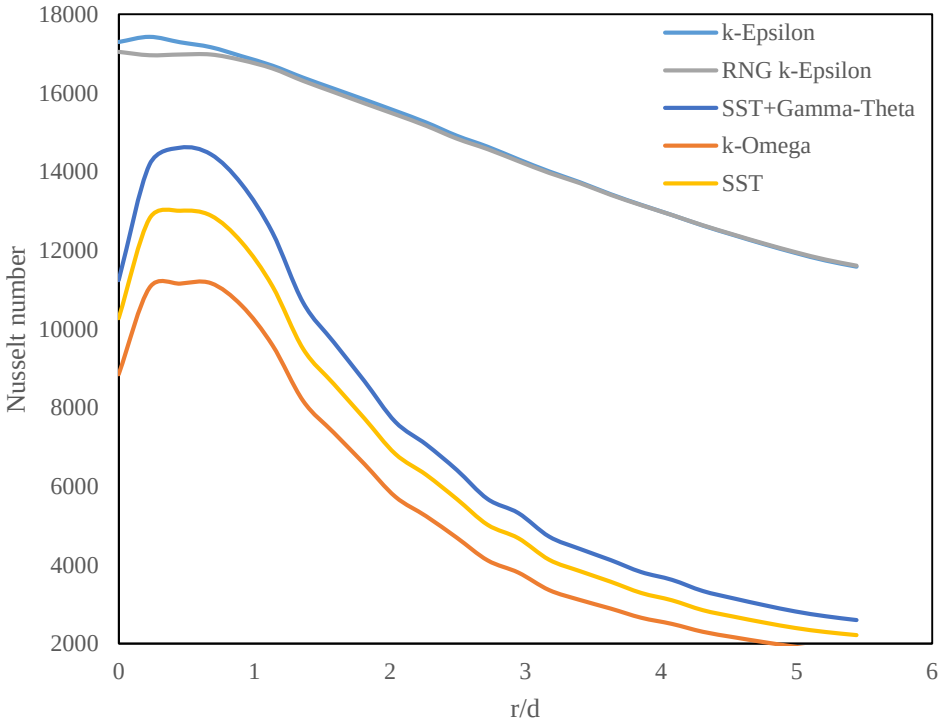

Fig. 4. Nusselt distribution at various turbulence models

Eq. (3) and Eq. (4) shows the SST equation which uses $(1 - F_t)$ term to reduce fluctuations. Also Eq. (5) and Eq. (6) shows the Gamma and Theta equation respectively which induces proper effect of intermediacy and onset transition.

$$\frac{\partial(\rho K)}{\partial t} + \frac{\partial(\rho U_j K)}{\partial x_j} = \frac{\partial}{\partial x_j}\left\{[\mu + \sigma_k \mu_t]\frac{\partial K}{\partial x_j}\right\} + P_k - \beta\rho K\omega \quad (3)$$

$$\frac{\partial(\rho\omega)}{\partial t} + \frac{\partial(\rho U_j \omega)}{\partial x_j} = \frac{\partial}{\partial x_j}\left\{\left[\mu + \frac{\mu_t}{\sigma_\omega}\right]\frac{\partial \omega}{\partial x_j}\right\} + 2(1 - F_t)\rho\frac{1}{\rho_{\omega 2}}\frac{\partial K}{\partial x_j}\frac{\partial \omega}{\partial x_j} + \alpha_3\frac{\omega}{K}P_k - \beta\omega\rho^2 \quad (4)$$

where,

K: Kinetic energy
ρ: Density of fluid
U: Velocity component in corresponding direction
μ_t: Eddy viscosity

$$\frac{\partial(\rho\gamma)}{\partial t} + \frac{\partial(\rho U_j \gamma)}{\partial x_j} = \frac{\partial}{\partial x_j}\left\{\left[\mu + \frac{\mu_t}{\rho}\right]\frac{\partial \gamma}{\partial x_j}\right\} + P_k - E_\gamma \quad (5)$$

$$\frac{\partial(\rho Re_{\theta t})}{\partial t} + \frac{\partial(\rho U Re_{\theta t})}{\partial x_j} = \frac{\partial}{\partial x_j}\left\{\sigma_{\theta t}(\mu + \mu_t)\frac{\partial Re_\theta}{\partial x_j}\right\} + P_{\theta t} \quad (6)$$

where,
P_k: Turbulence production
E_γ: Dissipation
$P_{\theta t}$: Controls the flow in the boundary layer

The solver makes use of continuity equation (Eq. (7)) and momentum equation (Eq. (8)) along with energy equations for accurately predicting the heat transfer phenomenon.

$$\frac{\partial \rho}{\partial t} + \nabla(\rho.\vec{v}) = S_m \quad (7)$$

$$\frac{\partial \vec{v}}{\partial t} + \nabla(\rho.\vec{v}.\vec{v}) = -\Delta p + \Delta\bar{\bar{\tau}} + \rho.\vec{g} + \vec{f} \quad (8)$$

where,
Δp: Change in pressure
$\Delta\bar{\bar{\tau}}$: Change in shear stress

2.3 Validation of Turbulence Modelling

The use of SST + Gamma-Theta model is validated using the results of the previous studies [17-18]. Simulations are carried out for Re = 50, 150, 200 and 500 along with z/d = 2, 3, 6 and 8. Nusselt distributions are obtained and plotted against r/d. Also, the Nusselt values fetched from previous studies [17-18] are plotted on the same plots. Figure 5 shows the numerical values along with the values from previous studies [17-18]. The deviation of numerical values with respect to results from previous studies [17-18] is very minor. Thus, the use of SST + gamma-Theta model is justified.

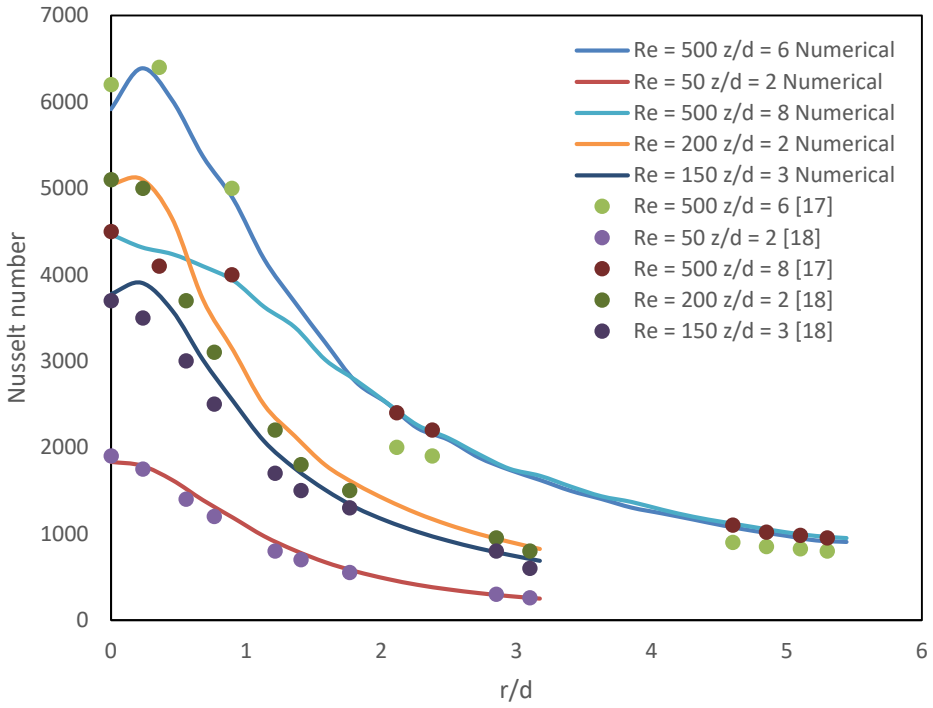

Fig. 5. Validation of turbulence model with previous studies [17-18]

3. Results

In order to develop semi-empirical relations representing STDEV against constant C = Re/ (z/d), Nusselt profiles are plotted against r/d for varying Reynolds number between 2000 and 3600 at z/d = 4 as well as for varying z/d from 1 to 8 at Re = 750. The standard deviation of local Nusselt magnitudes are then evaluated from the corresponding Nusselt profile.

3.1 Nusselt Profile for Varying Reynolds Number

Figure 6 shows the variation in the local Nusselt magnitude at Reynolds number 2000, 2200, 2400, 2600, 2800, 3000, 3200 and 3400 at constant z/d = 4. The Nusselt magnitude initially increases in the near stagnation region (0 < r/d < 1) and then it decreases gradually. Thus giving rise to secondary peaks in the Nusselt distribution. The secondary peaks are observed due to stretching of skin in the transition region. The standard deviation of Nusselt values are then obtained using the distribution.

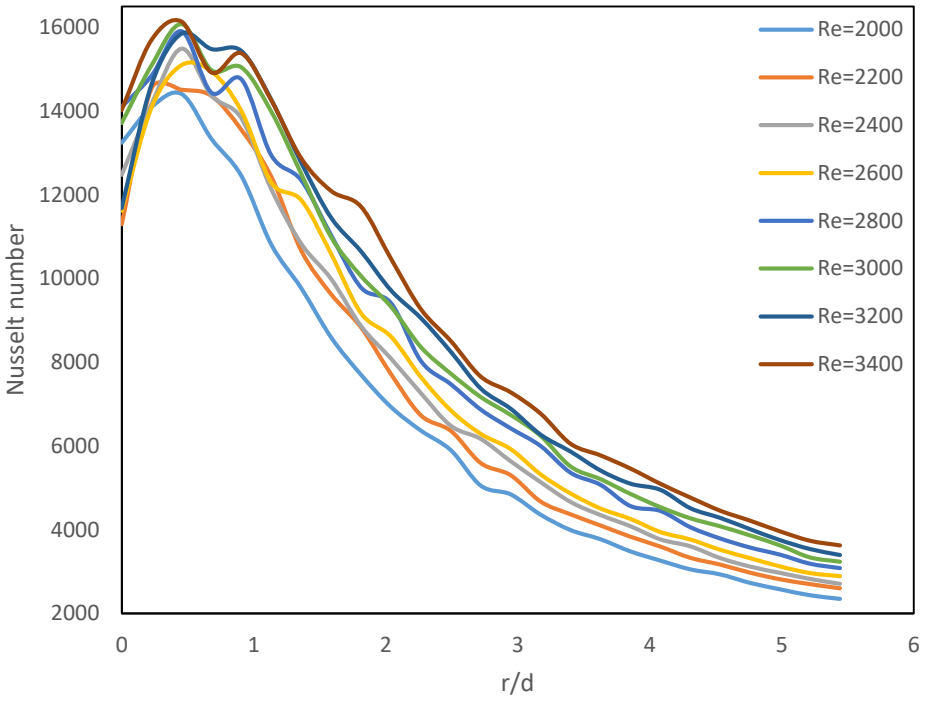

Fig. 6. Nusselt profile at varying Reynold number and z/d = 4

3.2 Nusselt Profile for Varying z/d

The variation in Nusselt distribution at z/d = 1, 2, 3, 4, 5, 6, 7 and 8 with Reynolds number kept constant at 750 are shown in Figure 7. The secondary peaks are present in the Nusselt distribution at lower z/d and diminishes as z/d increases. Local Nusselt magnitude is evaluated against r/d and then with the help pf local Nusselt magnitude the standard deviation of the local Nusselt magnitude at varying z/d is evaluated.

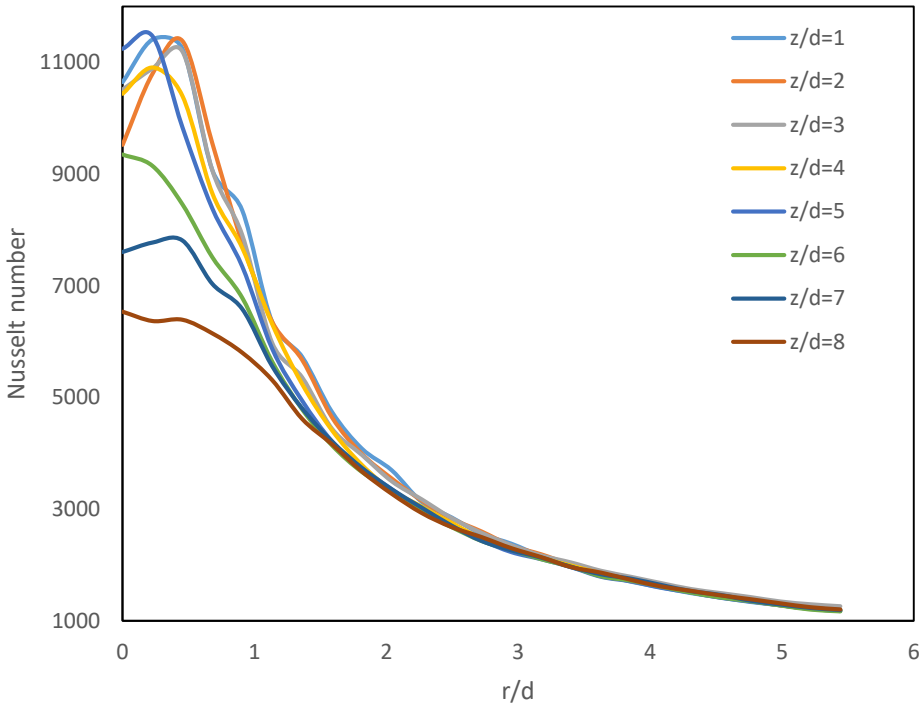

Fig. 7. Nusselt profile at varying z/d and Re = 750

3.3 Development of Semi-Empirical Relation Representing STDEV

The standard deviation (STDEV) of local magnitudes obtained at varying Reynolds number and varying z/d ratio are plotted in Figure 8 against constant C. The distribution of STDEV increases gradually up to C = 200 and then remains constant as the Nusselt distribution follows similar pattern at increasing z/d. Therefore, using regression analysis, correlation representing STDEV as a function of C is evaluated up to C = 200 (Eq. (9)).

$$STDEV = 14.751 \times (C)^{0.917} \tag{9}$$

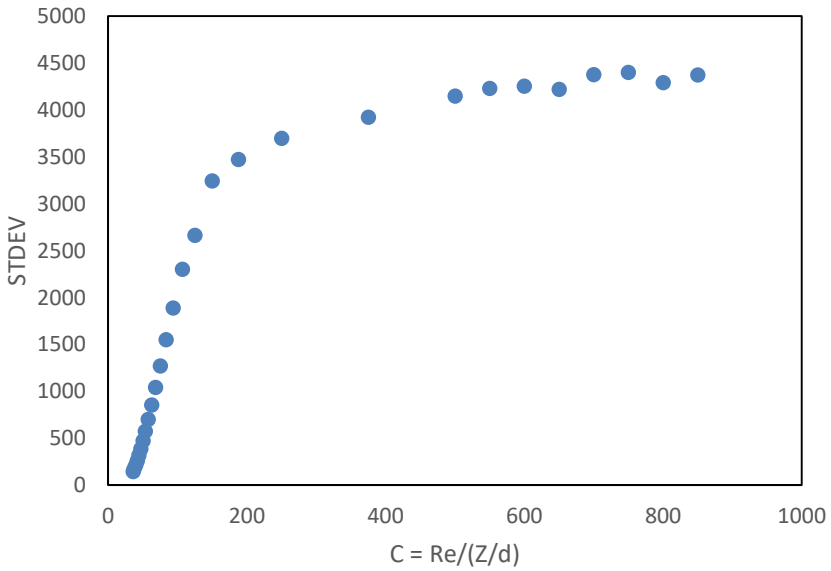

Fig. 8. Standard deviation (STDEV) v/s Constant (C = Re/ (z/d))

3.4 Validation of Semi-Empirical Relation Representing STDEV

The parameters Reynolds number and z/d from previous studies [17-18] are substituted in Eq. (9) in order to obtain the STDEV from correlation. Also, the STDEV from results of previous studies [17-18] are fetched and plotted against correlation STDEV values (Figure 9). The best fit line of STDEV is added in the graph and the closeness of the results with the best fit line validates the semi-empirical relation representing STDEV (Eq. (9)).

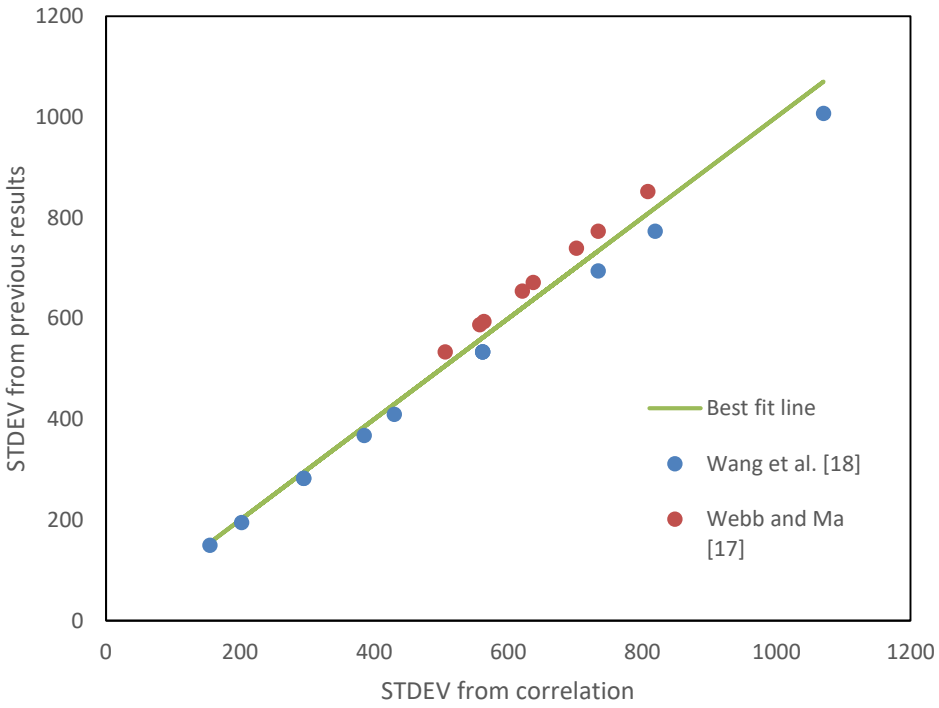

Fig. 9. Validation of semi-empirical relation representing STDEV with previous results [17-18]

4. Conclusions

An independent grid size having minimum and maximum face size of 8.57×10^{-5} and 8.57×10^{-3} respectively with 1.05 is evaluated. SST + Gamma-Theta turbulence model is found to predict the most accurate results among all the turbulence models used. Using local Nusselt magnitudes at varying Reynolds number and z/d ratio, the correlation representing STDEV is proposed in terms of C successfully as $STDEV = 14.751 \times (C)^{0.917}$. Also, the correlation is validated using results of previous studies.

References

[1] Umair, S. Mohd, and N. Parashram Gulhane. "Numerical investigation of non-dimensional constant representing the occurrence of secondary peaks in the Nusselt distribution curve." *International Journal of Engineering TRANSACTIONS A* 29 (2016): 1453-1461.

[2] Umair, Siddique Mohd, and Nitin Parashram Gulhane. "On numerical investigation of heat transfer augmentation through pin fin heat sink by laterally impinging air jet." *Procedia Engineering* 157 (2016): 89-97.

[3] Umair, Siddique Mohd, and Nitin Parashram Gulhane. "On numerical investigation of non-uniformity in cooling characteristic for different materials of target surfaces being exposed to impingement of air jet." *International Journal of Modeling, Simulation, and Scientific Computing* 8, no. 03 (2017): 1750024.

[4] Umair, Siddique Mohammed, Abhijeet Rangnath Kolawale, Ganesh Anurath Bhise, and Nitin Parashram Gulhane. "On numerical heat transfer characteristic study of flat surface subjected to variation in geometric thickness." *International Journal of Computational Materials Science and Engineering* 6, no. 02 (2017): 1750010.
[5] Siddique, Umair M., Ganesh A. Bhise, and Nitin P. Gulhane. "On numerical investigation of local Nusselt distribution between flat surface and impinging air jet from straight circular nozzle and power law correlations generation." *Heat Transfer—Asian Research* 47, no. 1 (2018): 126-149.
[6] Umair, Siddique Mohammed, Abdulrahman Alrobaian, Sher Afghan Khan, Marthande Gnanagonda Kashinath, and Patil Rajesh. "Numerical Investigation of Critical Range for the Occurrence of Secondary Peaks in the Nusselt Distribution Curve." *CFD Letters* 10, no. 2 (2018): 1-17.
[7] Siddique, Umair M., Gulhane P. Nitin, Sher A. Khan, Jan Taler, Arthur Cebula, Pawel Oclon, and Rajesh Patil. "Numerical investigation of semiempirical relations representing the local Nusselt number magnitude of a pin fin heat sink." *Heat Transfer—Asian Research* 48, no, 5 (2019): 1857-1888.
[8] Mohd Umair, S., N. P. Gulhane, A. R. A. Al-Robaian, and S. A. Khan. "On Numerical Investigation of Semi-empirical Relations Representing Local Nusselt Number at Lower Nozzle-target Spacing's." *International Journal of Engineering* 32, no. 1 (2019): 137-145.
[9] Umair, Siddique Mohd, Sher Afghan Khan, Abdulrahman Alrobaian, and Emaad Ansari. "Numerical Study of Heat Transfer Augmentation Using Pulse Jet Impinging on Pin Fin Heat Sink." *CFD Letters* 11, no. 3 (2019): 84-91.
[10] Dobbertean, Mark Michael. "Steady and Transient Heat Transfer for Jet Impingement on Patterned Surfaces." PhD diss., M. Sc. thesis, Department of Mechanical Engineering, (2011).
[11] Sher Afghan Khan, Abdulrahman A. Alrobaian, Mohammed Asadullah, and Aswin. "Threaded Spikes for Bluff Body Base Flow Control." *Journal of Advanced Research in Fluid Mechanics and Thermal Sciences* 53, no. 2 (2019): 194-203.
[12] Khan, Sher Afghan, Abdulrahman Abdullah Al Robaian, Mohammed Asadullah, and Abdul Mohsin Khan. "Grooved Cavity as a Passive Controller behind Backward Facing Step." *Journal of Advanced Research in Fluid Mechanics and Thermal Sciences* 53, no. 2 (2019): 185-193.
[13] Pathan, Khizar Ahmed, Prakash S. Dabeer, and Sher Afghan Khan. "Investigation of Base Pressure Variations in Internal and External Suddenly Expanded Flows using CFD analysis." *CFD Letters* 11, no. 4 (2019): 32-40.
[14] Pathan, Khizar Ahmed, Prakash S. Dabeer, and Sher Afghan Khan. "Influence of Expansion Level on Base Pressure and Reattachment Length." *CFD Letters* 11, no. 5 (2019): 22-36.
[15] Sajali, Muhammad Fahmi Mohd, Syed Ashfaq, Abdul Aabid, and Sher Afghan Khan. "Simulation of Effect of Various Distances between Front and Rear Body on Drag of a Non-Circular Cylinder." *Journal of Advanced Research in Fluid Mechanics and Thermal Sciences* 62, no. 1 (2019): 53-65.
[16] Khan, Sher Afghan, Abdul Aabid, Fharukh Ahmed Mehaboobali Ghasi, Abdulrahman Abdullah Al-Robaian, and Ali Sulaiman Alsagri. "Analysis of area ratio in a CD nozzle with suddenly expanded duct using CFD method." *CFD Letters* 11, no. 5 (2019): 61-71.
[17] Webb, B. W., and C-F. Ma. "Single-phase liquid jet impingement heat transfer." In *Advances in heat transfer* 26, (1995): 105-217.
[18] Wang, Hemu, Wei Yu, and Qingwu Cai. "Experimental study of heat transfer coefficient on hot steel plate during water jet impingement cooling." *Journal of Materials Processing Technology* 212, no. 9 (2012): 1825-1831.